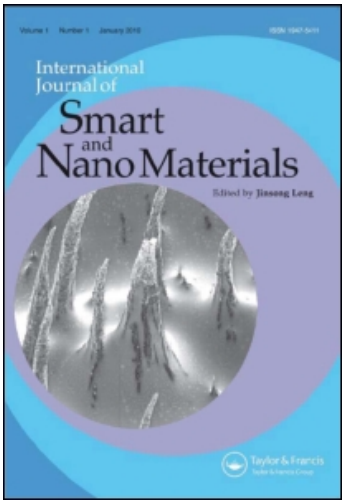

International Journal of Smart and Nano Materials
Publication details, including instructions for authors and subscription information:
http://www.informaworld.com/smpp/title~content=t910571122

EMI shielding effectiveness of silver nanoparticle-decorated multi-walled carbon nanotube sheets

Wenming Zhao[a]; Mei Li[b]; Zhongyi Zhang[c]; Hua-Xin Peng[a]
[a] Advanced Composites Centre for Innovation and Science (ACCIS), Department of Aerospace Engineering, University of Bristol, Queens Building, Bristol, UK [b] School of Chemistry, University of Bristol, Bristol, UK [c] Mechanical & Design Engineering, University of Portsmouth, Portsmouth, Hants, UK

First published on: 23 November 2010

To cite this Article Zhao, Wenming , Li, Mei , Zhang, Zhongyi and Peng, Hua-Xin(2010) 'EMI shielding effectiveness of silver nanoparticle-decorated multi-walled carbon nanotube sheets', International Journal of Smart and Nano Materials, 1: 4, 249 — 260, First published on: 23 November 2010 (iFirst)
To link to this Article: DOI: 10.1080/19475411.2010.511477
URL: http://dx.doi.org/10.1080/19475411.2010.511477

International Journal of Smart and Nano Materials
Vol. 1, No. 4, November 2010, 249–260

EMI shielding effectiveness of silver nanoparticle-decorated multi-walled carbon nanotube sheets

Wenming Zhao[a], Mei Li[b], Zhongyi Zhang[c] and Hua-Xin Peng[a]*

[a]*Advanced Composites Centre for Innovation and Science (ACCIS), Department of Aerospace Engineering, University of Bristol, Queens Building, Bristol, BS8 1TR, UK;* [b]*School of Chemistry, University of Bristol, Bristol, BS8 1TS, UK;* [c]*Mechanical & Design Engineering, University of Portsmouth, Portsmouth, Hants, PO1 3DJ, UK*

(*Received 5 June 2010; final version received 23 July 2010*)

With the aim of exploring the excellent properties of multi-walled carbon nanotubes (MWNTs) in modern composite technologies, various macrostructures of nanotubes have been developed from one to three dimensions, e.g. fibers, networks, sheets (buckypapers) and pellets. The MWNT sheets discussed here were fabricated by a vacuum filtration procedure, a process that has potential for large-scale manufacturing. In order to further enhance the transport properties of MWNT sheets by reducing the contact resistance between nanotubes, highly conductive silver nanoparticles were introduced by an *in situ* photochemical reduction method. TEM analysis showed that highly acid-treated MWNTs dispersed in the presence of Triton X-100 (TX-100) under UV light was a controllable processing method for preparation of a narrow size distribution of silver nanoparticles that were anchored onto the nanotubes. The free-standing MWNT/Ag nanohybrid sheets possessed a sharp increase in electrical conductivity from 27.7 to 40.0 S/cm, which consequently led to a much improved electromagnetic interference shielding effectiveness (SE). In principle, the SE could reach 3500 dB/cm with a thickness of 110 μm, which matched the experimental results well. In addition, the nanohybrid sheets are robust and can be folded with a thickness of 30 μm, which opens a promising way to integrate MWNT sheets into conventional composite laminates.

Keywords: carbon nanotube; silver nanoparticle; electromagnetic shielding effectiveness; nanohybrid

1. Introduction

In order to fully explore the excellent properties of carbon nanotubes (CNTs), work in the past has been focused on generating CNTs networks, films and sheets (buckypaper) using spraying or the vacuum filtration method [1,2] on solid substrates or by integration with polymers. Compared with single-walled carbon nanotubes (SWNTs), multi-walled carbon nanotubes (MWNTs) are much cheaper and better suited to large-scale industrial applications except for their much lower conductivity compared with SWNTs. There have been several strategies to reduce their high contact resistance, including chemical doping, alignment and welding with metals or conducting polymers. Dai [3] reported that chemical doping leads to orders of magnitude reduction in the resistance of bulk SWNT

*Corresponding author. Email: h.x.peng@bristol.ac.uk

ISSN 1947-5411 print/ISSN 1947-542X online

DOI: 10.1080/19475411.2010.511477
http://www.informaworld.com

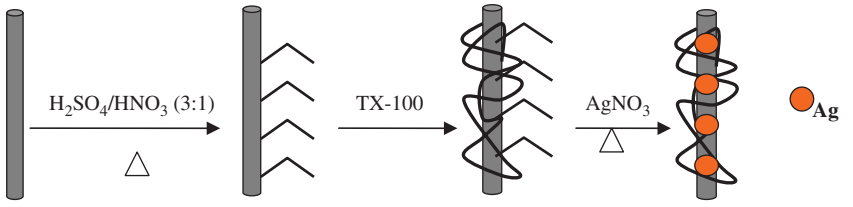

Figure 1. Schematic illustration of the process of synthesizing and anchoring silver nanoparticles onto MWNTs.

materials due to the increase in the average number of hole or electron carriers in the nanotubes. For both SWNT and MWNT sheets, there are two predominant nanotube junctions that govern the electrical properties of a nanotube network, i.e. the Y junction, exhibiting ambipolar behavior, and the crossed junction, providing rectification characteristics [4]. Therefore, two approaches can be used to improve the electrical conductivity of MWNT sheets: (1) minimize the contact resistance between nanotubes by improving the alignment of nanotubes and by increasing the lengths of individual tubes; (2) improve the conductivity of individual nanotubes by post-synthesis treatments [5]. To achieve low-resistance ohmic contacts in these structures, metals can be deposited onto the nanotube surface by using techniques such as impregnation [6], electroless metal plating [7], self-assembly [8], electrodeposition [9], and physical vapor deposition [10], etc.

In the present work, MWNTs were grafted with carboxylic groups by boiling MWNTs in a strong acid mixture of H_2SO_4/HNO_3 (3:1). Highly conductive silver nanoparticles were then *in situ* synthesized and anchored onto the MWNT surface by photochemical reduction of $AgNO_3$ in the presence of Triton X-100 (TX-100) surfactant, as shown in Figure 1. The nanohybrid suspension was then filtered using a vacuum filtration procedure to fabricate uniformly distributed MWNT sheets. The effect of silver nanoparticles on the electrical properties and electromagnetic interference (EMI) shielding effectiveness was investigated.

2. Experimental details

The pristine MWNTs (Sigma Aldrich) were produced using a chemical vapor deposition (CVD) method (a purity of $> 99\%$), with up to 20 μm in length and a diameter around 12 nm. Pristine MWNTs (4.32 g) were added to 120 ml of concentrated acid mixture ($H_2SO_4/HNO_3 = 3{:}1$ by volume). The mixture was placed in an ultrasonic bath (40 kHz) for 30 min and then stirred for 4 h at 100°C. The mixture was then diluted with distilled water and no sedimentation was noticed after leaving it overnight. The resulting solution was then vacuum filtered through a 0.22 μm Millipore alumina membrane and subsequently washed with distilled water until the pH value was $\sim$7. The filtered solid was dried under vacuum for 24 h at 40°C, yielding 2.59 g carboxylic-modified MWNTs (MWNT-COOH). Acid-treated MWNTs (100 mg) were then dispersed in distilled water in the presence of TX-100 surfactant (1.0 wt %), and then mixed with silver nitrate solution (250 ml, 0.2 wt %), while stirring under UV light ($\lambda = 365$ nm) at 60°C. The nanohybrid sheets were fabricated by filtering the above mixture through Millipore filter and subsequently washed with distilled water and ethanol.

A zeta potential analyzer was used to measure the zeta potential and mobility of the resulted carboxylic-modified MWNTs. Scanning electron microscopy (SEM) was used

to characterize the morphologies of the as-synthesized MWNTs. SEM was performed using a JEOL 1530 equipped with a thermally assisted field emission gun operating at 10 keV. The morphology of silver nanoparticles stabilized by MWNTs was further examined by transmission electron microscopy (TEM, JEOL 1200). To prepare the TEM samples, a tiny drop of well-dispersed sample was placed onto one carbon-coated TEM copper grid. Fourier-transform infrared (FTIR) spectroscopy was utilized to study the acid-treated MWNTs. The acid-treated MWNTs were mixed with dried KBr powder and pressed to form semi-transparent pellets.

Electrical conductivity measurements were conducted using the four-probe method (a 4284A Precision LCR meter) at room temperature. The transmission and reflection characteristics of MWNT sheets toward EMI were measured by using a vector network analyzer (VNA) with a band range up to 50 GHz together with a pair of horn antennas with a band range of 15–40 GHz.

3. Results and characterizations

3.1. Ag nanoparticle-decorated MWNT sheets

It was found that the MWNT sheets (>30 mg) could be easily separated from alumina membranes above a certain thickness with adequate conductive properties and mechanical strength. Figure 2 shows that MWNT sheets prepared using the vacuum filtration method were predominantly cylindrical, and occasionally the resulting MWNT sheets appeared oval or had roughened edges, but the overall upper and lower surfaces of the MWNT sheet appeared to be flat. The diameter after contraction varied depending on the various types of solvents used as dispersion medium. For distilled water, the average contraction ratio of the MWNT sheets was up to ∼10% in diameter and formed domed shaped MWNT sheets that possess a concave upper surface and convex lower surface, as shown in Figure 2. During drying shrinkage, MWNT sheets were found to separate from the alumina filter automatically, the mechanism of which can be well understood based on Kendall's theory [11]. Kendall suggested that shrinkage weakens joints between the nanotube sheet and the alumina membrane. The thickness limitation is probably due to the difficulty in forming an intact film across a substrate comprising large-sized pores and its subsequent removal from the frit surface.

Figure 3a shows an optical image of the stable carboxylic-modified MWNTs in aqueous solutions after two months and it was found that better dispersion could be obtained in a solution with mean zeta potential of −34.03 mV and mobility of $-2.66(\mu/s)/(V/cm)$.

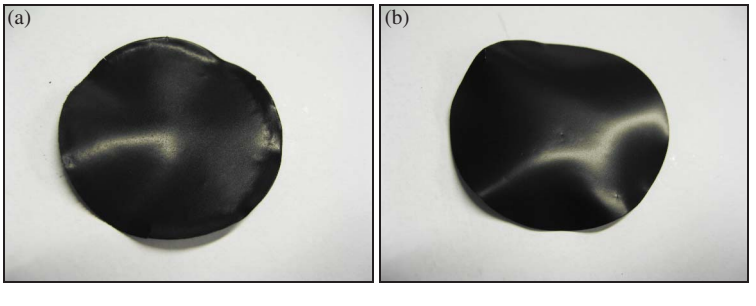

Figure 2. Surface morphology of silver-decorated MWNTs sheets with a thickness of 30 μm: (a) front view and (b) backside view.

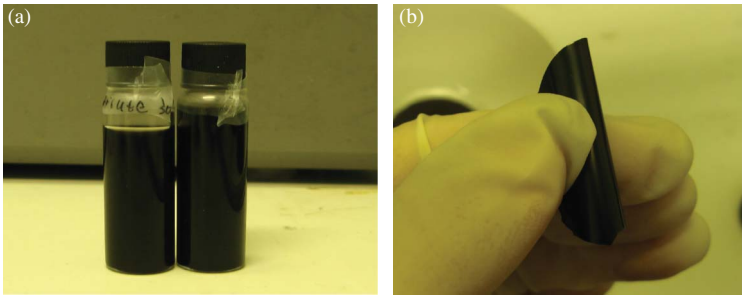

Figure 3. Photographs of (a) stable acid-treated MWNTs in aqueous solutions after two months (left: dilute; right: concentrated) and (b) the foldability evaluated by measuring bending radius of 1.5 mm (approximate tensile strain of 6.5%).

The monodispersed nanotube solution yielded a higher concentration of crosslink joints, and thus a higher bending modulus [12] and much more conductive tunnels. Figure 3b indicates that a foldable free-standing MWNT sheet (Φ36 mm $\times$ 30 μm) was condensed enough to exhibit a metal-like shiny surface, which is very rare for MWNT sheets. The degree of foldability was directly related to the size of the film. One measure of this could be the curvature of the film, which is worth further investigation.

3.2. Zeta potential and UV–visible spectra

Particle surface charge is an important feature that determines colloidal stability. The electrostatic potential of charged particles dispersed in a liquid medium is governed mainly by surface functionality, especially by its ionization ability to produce a charged surface, and the preferential absorption of ions of one charge sign from solution. Zeta potential measurements were performed to detect the influence of various chemical modifications on MWNT surface, charged in an aqueous solution. Generally, particles tend to avoid coagulation by electrostatic repulsion above certain surface potentials, usually $\pm$ 15 mV [13]. Thus, by knowing the magnitude of the net surface potential, one can predict the possible aggregation behavior of MWNTs. For example, a high surface charge on nanotube surface will indicate a preference for considerable electrostatic repulsion within nanotube aggregates. A low surface charge may not be able to overcome the van der Waals forces between tubes, and hence lead to a high degree of aggregation. But particles with zeta potentials between -15 and $+15$ mV can still be stable if they are stabilized sterically.

Table 1 shows that carboxylic-modified and surfactant-modified MWNTs are negatively charged in aqueous solution, and colloidal stability is fully correlated with the surface functionality. Thus, TX-100-modified nanotubes are stabilized in solution primarily by steric and not electrostatic interactions. However, carboxylic-modified MWNTs showed a higher surface charge, as the ionization reaction of carboxylic acids

Table 1. Mobility and zeta potential of aqueous solution of MWNTs with 1.0 wt % surfactant.

Sample	Mobility	Zeta potential (mV)
MWNT-TX-100	-1.76	-22.57
Acid-treated MWNT	-2.66	-34.03

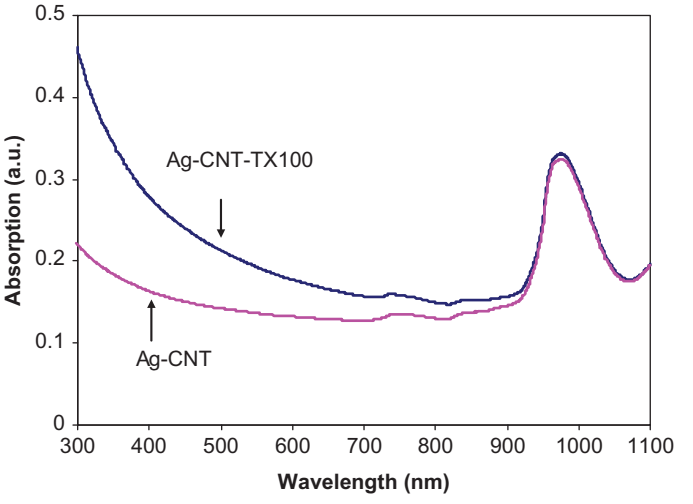

Figure 4. UV–visible spectroscopy of the dispersed silver/MWNTs suspension with and without the surfactant TX-100.

in water is sufficiently effective ($4 < pK_a < 5$). According to the well-established Derjaguin–Landau–Verwey–Overbeek (DLVO) theory, particles can be dispersed when electrostatic repulsions, induced by similarly charged electrical layers surrounding the particles, can overcome the attractive van der Waals' interactions [14]. The net interaction between nanotubes is obtained by summing these two terms. If the repulsion potential exceeds the attraction potential, an energy barrier that opposes aggregation occurs. If the magnitude of this energy barrier exceeds the kinetic energy of the particles, the suspension is stable. The relatively high zeta potential of carboxylic-modified MWNTs (−34 mV) in water increases the energy barrier for coagulation and contributes to stable dispersions of this type of nanotube in aqueous solution, and eventually leads to homogenized composite-film formation.

To further support the observation that dispersions of individual Ag-decorated MWNTs are basically free of bundles, UV–visible absorption spectra of such dispersions were obtained. It has been previously reported that such spectra are very sensitive to the aggregation state of nanotubes in a suspension [15]. Figure 4 shows the UV–visible absorption spectra in the range 300–1100 nm. The UV–visible–NIR spectra exhibited sharp features corresponding to electronic transitions between the MWNT Van Hove singularities. The observation of pronounced spectral features suggests the presence of individual MWNTs in solution, since bundling would lead to a broadening of the absorption spectra.

3.3. FTIR analysis of the carboxylic-modified MWNTs

In order to characterize the attachment of carboxylic acid groups on the nanotube surface, the FTIR spectra of the pristine and carboxylic-modified MWNTs were obtained, as shown in Figure 5. The dominant peak at 1626 cm^{-1} can be assigned to characterize acid carbonyl (C=O) stretches, and the broad band at 3417 cm^{-1} is identified as O–H stretching mode in carboxylic acid groups. The peak at 1584 cm^{-1} is attributed to the vibration of carbon skeleton of the nanotubes. The results indicated that carboxylic acid groups had been successfully attached to the nanotubes.

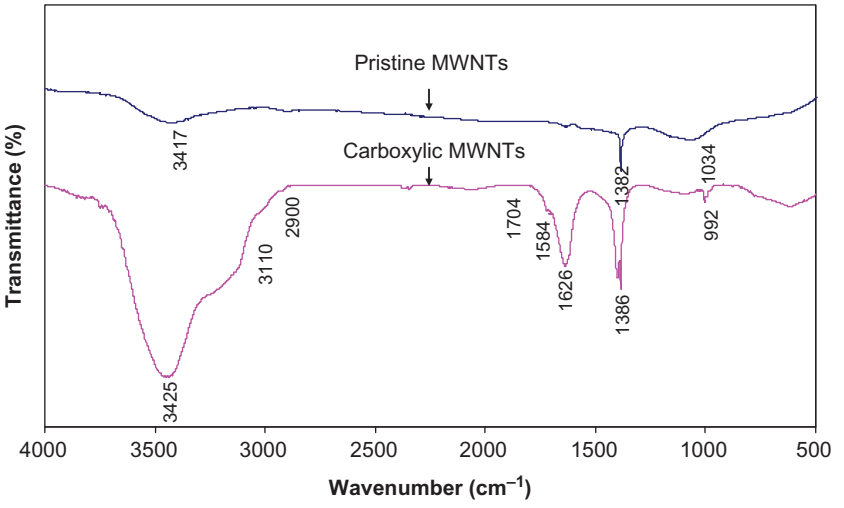

Figure 5. FTIR spectra of pristine MWNTs and acid-treated MWNTs.

3.4. TEM images of silver-decorated MWNTs

Figure 6a shows a TEM image of Ag nanoparticles synthesized by using carboxylic-modified MWNTs as stabilizing agent without TX-100 surfactant. With nanotubes as backbone, silver nanoparticles lined up to form a stable assembly, which also indicated that active sites on the carboxylic-modified MWNTs walls aided the nucleation and growth of Ag particles. However, the particles or agglomerations had quite a broad size distribution, from 10 to 100 nm, with hexagonal, pentagonal and spherical shapes. Also, the nanoparticles can only anchor onto certain nanotubes, implying an inhomogeneous distribution of the nanoparticles (NPs) in the future MWNT/NP sheet. However, it is evident from above analysis that the acid-treated MWNTs were considerably effective in stabilizing silver nanoparticles. The stabilizing mechanism was proposed as the following: the oxygen elements on the acid-treated MWNTs walls provided the nucleation sites for metal ions and then stabilized the nanoparticles after they were formed. MWNTs acted as the template on which the as-formed nanoparticles were able to line up to form a stable assembly due to their special structures [16].

From above analysis, one can see that whereas carboxylic-modified MWNTs could supply nucleation sites for Ag nanoparticles, the particle size could not be effectively controlled during the process. TX-100 can not only act like surfactant but can help control the particle size, as well as acting as a reducing agent at the same time [17]. For silver nanoparticles synthesized by using the same amount of acid-treated MWNTs in the presence of 1 vol. % of TX-100, the silver NPs were stabilized on the nanotube wall and well dispersed with a narrow size distribution, as can be seen in Figure 6c. For a ratio of 1:1 $AgNO_3$/MWNTs, the percentage in the range 20–30 nm was 66% and the maximum particle size was around 40 nm. This indicated that TX-100 is efficient in controlling the particle size and distribution by preventing agglomeration. Although the TEM samples were prepared by dispersing the nanohybrid suspensions by strong sonication, nanotubes were still tightly connected by nanoparticles and conducting paths were thus set up, which enhanced the transport properties of the nanotube sheets.

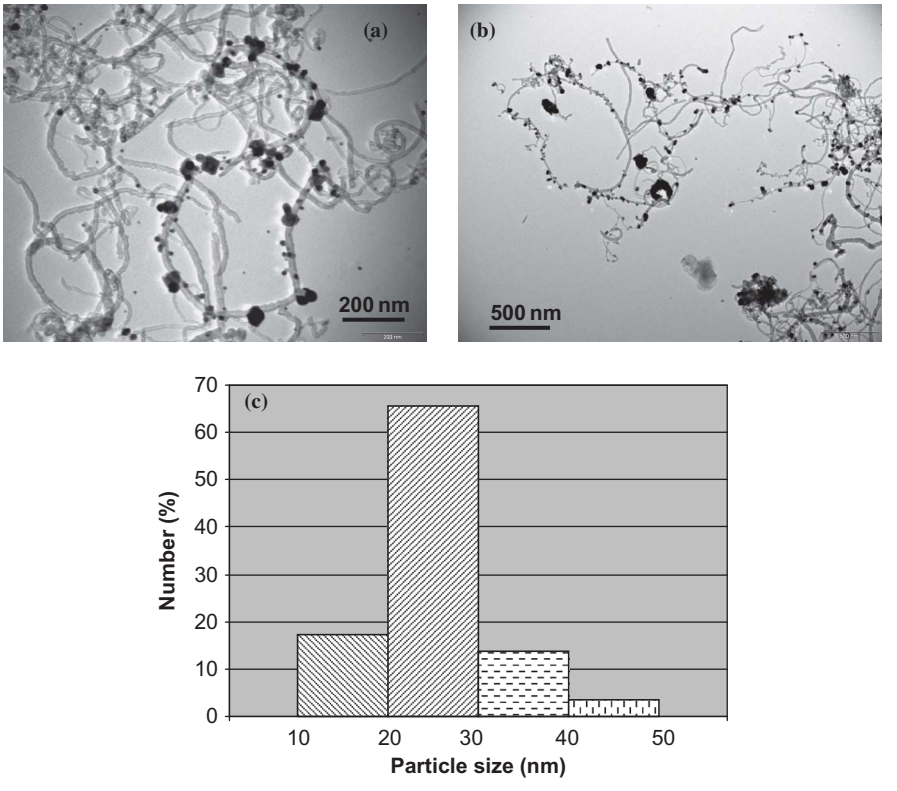

Figure 6. (a) TEM images of Ag particles synthesized by using acid-treated MWNTs, (b) TEM images of Ag/MWNT-COOH in the presence of TX-100 and (c) histograms of silver particles size distribution ($AgNO_3$/MWNTs = 1:1) in (b).

3.5. Microstructure of functionalized MWNT sheets

Figure 7 shows the typical microstructure of functionalized MWNT sheets. The MWNT sheets generally maintained a planar geometry along the upper surface, but individual nanotubes were randomly orientated throughout the bulk sample, predominantly lying parallel to the frit surface. Under a high magnification, the nanotube sheet surface was pitted

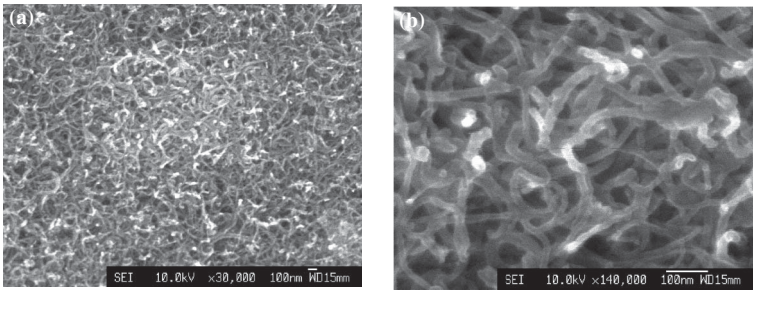

Figure 7. SEM images of MWNT sheets at magnifications of (a) ×30,000 and (b) ×140,000.

with numerous micron-sized holes, presumably where the nanotubes were forced into the interstices of the frit surface, giving the surface a roughened morphology. It is assumed that by reducing the porosity of the frit, it should be possible to reduce the level of voids, although this may increase the time required for the solvent to escape the system under compression. This also proved to be useful for casting thinner MWNT sheets for more flexible applications. A closer SEM examination (Figure 7b) revealed that the surface of MWNT sheets was in fact rather rough, and the tubes formed a random, heavily interconnected macroporous system. Their dominant orientation was normal to the direction of the filtration, without any bundling. By quantitatively analyzing the SEM images, the apparent pore diameter was 30–50 nm. The nominal density of the nanotube sheet is $0.56 g/cm^3$ and the average porosity is 68.8%, together with a surface area of $112.11\ m^2/g$ determined by the BET method.

3.6. Thermal stability of Ag/MWNT hybrid sheets

In order to assess the activity of the acid-treated MWNTs and the percentage of Ag nanoparticles in the resulting nanohybrid sheets, thermogravimetric analysis (TGA) of carboxylic-modified MWNT and Ag/MWNT hybrid sheets was carried out. Figure 8a shows that the main loss peaks occurred at 595 and 450°C. Above 600°C, almost nothing was left of the carboxylic MWNT sample, whereas 35.0 wt % still remained for Ag/MWNT hybrid sample. The silver oxides (Ag_2O) remained brown in color and were sintered into large particles during the melting process, as shown in Figure 8b. By calculating the percentage of silver in Ag_2O ($215.6/231.6 = 0.931$), totally 32.5 wt % of silver NPs were deposited onto MWNTs. The TGA curves also showed that the main decomposition peak of MWNTs shifted to a lower temperature range, most likely due to the formation of a silver shell around the nanotubes [18].

3.7. Electromagnetic interference (EMI) shielding effectiveness

The electrical resistance of MWNT sheets is derived from two components: the resistance of individual nanotubes and the contact resistance between nanotubes. The decorated Ag nanoparticles appear to further increase the carrier density, leading to an increasing in conductivity from 27.7 to 40.0 S/cm, as shown in Table 2. Based on the theory of EMI shielding, the shielding effectiveness (SE) is described as [5]

$$\mathrm{SE} = 20 \log \left| (1/4n)[(1+n)^2 \exp(-ikd) - (1-n)^2 \exp(ikd)] \right|, \tag{1}$$

where the complex index of refraction n is related to the complex wave vector k ($= n\omega/c$). Under a good conductor approximation, the SE of monolayer films described in the above equation is given as follows [19]:

$$\begin{aligned} \mathrm{SE}_{mono} = 10 \log \Bigg\{ \frac{1}{4} \Bigg[& \frac{\sigma}{2\omega\varepsilon_0} \left(\cosh \frac{2d}{\delta} - \cosh \frac{2d}{\delta} \right) \\ & + 2\sqrt{\frac{\sigma}{2\omega\varepsilon 0}} \left(\sinh \frac{2d}{\delta} + \sinh \frac{2d}{\delta} \right) \\ & + 2 \left(\cosh \frac{2d}{\delta} + \cosh \frac{2d}{\delta} \right) \Bigg] \Bigg\}, \end{aligned} \tag{2}$$

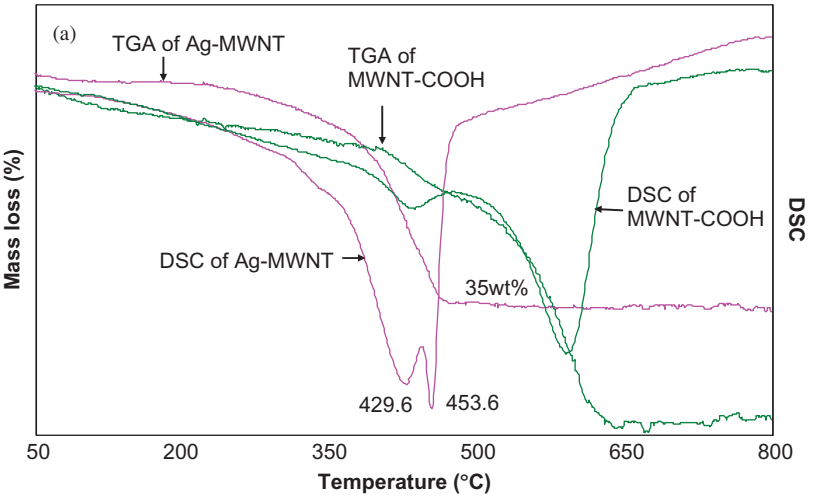

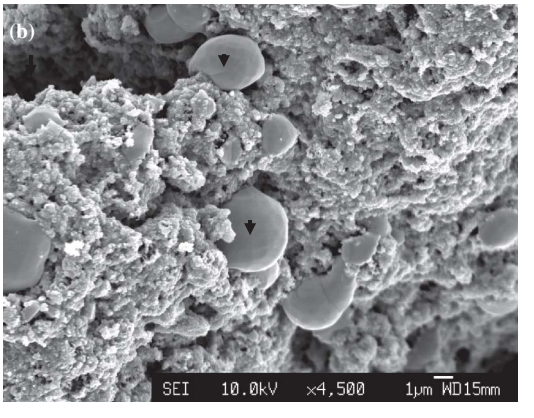

Figure 8. (a) TGA and DSC curves of carboxylic-modified MWNTs and MWNT/Ag nanohybrid sheets. (b) SEM image of MWNT/Ag remains after TGA testing, showing the large silver oxide particles, as indicated by arrows.

Table 2. Effect of Ag nanoparticles on the conductivity and EMI SE of MWNT sheets.

Material (monolayer)	σ (S/cm) (300 K)	Thickness (d) (μm)	SE (dB/cm)
MWNT/NPs	40	110	3500
MWNT	27.7	120	3005

where $\delta = \sqrt{2/\mu_0 \omega \sigma}$ is the skin depth. For an electrically thin shield ($d << \delta$), Equation (2) reduces to

$$\begin{aligned} \mathrm{SE} &\approx 20 \log \left(1 + \frac{Z_0 \sigma d}{2}\right) \\ &= 20 \log(\sigma d) + 20 \log \left(\frac{1}{\sigma d} + \frac{Z_0}{2}\right), \end{aligned} \tag{3}$$

where Z_0 (=376.7Ω) is the wave impedance of free space. The result shows that the EMI SE increases as σd increases, which means conductivity is an intrinsic parameter of EMI SE, and the thickness is an extrinsic parameter for EMI SE. As the thickness of the material increases, the EMI SE becomes larger due to the increasing of the absorption of the EM wave [20].

The transmission and reflection characteristics of MWNT sheets toward EMI were measured with a band range up to 50 GHz together with a pair of horn antennas with a band range of 15–40 GHz. A filter membrane was also analyzed under identical experimental conditions for comparison. During the EMI measurement, the carbon nanotube sheets were embedded between two layers of filter membrane, which has no influence on the EMI SE. The EMI SE curves are shown in Figure 9a, where the curve of the sample

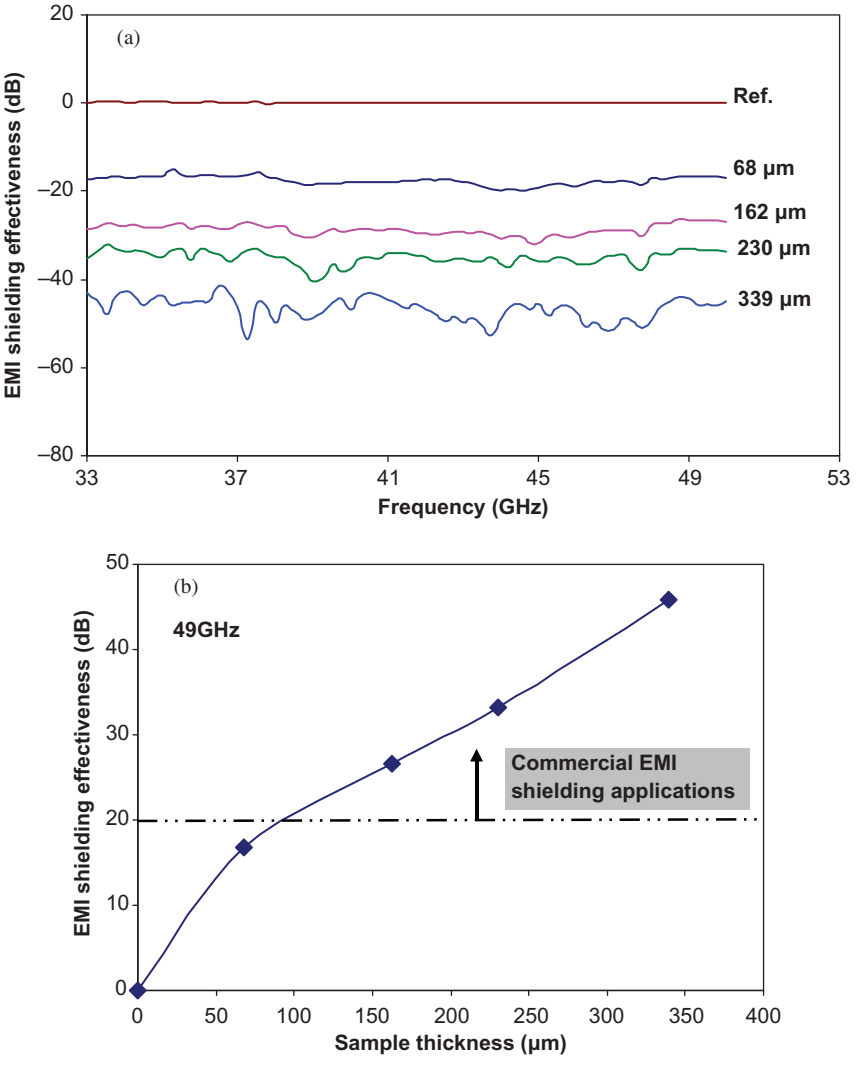

Figure 9. (a) EMI shielding effectiveness as a function of frequency measured in the 33–50 GHz range of different stacked layers of MWNT sheets. (b) Relationship between sample thickness and EMI shielding effectiveness at 49 GHz.

thicker than 339 μm is out of testing range according to the operation menu. There is a linear relationship between sample thickness and EMI SE value, as seen in Figure 9b. The EMI SE increases from 18.7 to 45.5 dB when the thickness of the nanotube sheets increases from 68 to 339 μm. With one layer of MWNT sheet with a thickness of 68 μm, the EMI SE increased dramatically and approached the target value (20.3 dB) of the EMI shielding materials needed for commercial applications [21].

For comparison with commercial metal mesh or metal films, Shui et al. compared the EMI shielding efficiency of a range of metal meshes and thin films. It was found that a single layer of MWNT sheet could achieve a higher EMI SE than the Ni mesh. Furthermore, for aerospace applications related to shielding or waveguides, the specific EMI SE and the specific surface conductance are the relevant quantities [22]. The specific SE value for MWNT sheet with a thickness of 68 μm was calculated to be 35.7 dB cm^3/g, which is much higher than that of typical metals, such as solid copper with a value of 10 dB cm^3/g [22]. The high SE of MWNT sheets is due to their small diameter, large aspect ratio, high conductivity, and the fact that the interaction of electromagnetic radiation with a conductor weakens with increasing depth from the surface of the conductor [23].

4. Concluding remarks

An environmental friendly method was developed to prepare monodispersed MWNT suspensions and synthesize Ag nanoparticles onto the carboxylic-modified MWNTs via an *in situ* synthesis procedure. The modification conditions of MWNTs were mild and the formation of MWNT/Ag nanohybrids was environmental friendly and well controllable. This strategy might also be suitable for the fabrication of MWNT/metal hybrids with many other metals (e.g. platinum, gold and binary metallic nanoparticles) for applications in nanoelectronics, biosensors, heterogeneous catalysis, electrocatalysis, optical devices, etc.

Silver nanoparticles were covalently anchored onto nanotube surface with a uniform distribution and the resulting silver junctions proved very promising for enhancing the transport properties between nanotubes. Stacked layers of thin nanotube sheets were very effective for absorbing EM waves, where an EMI SE value of 45 dB could be obtained with a stacked layers thickness of 339 μm. All these results demonstrate that the Ag nanoparticle-decorated MWNT sheets are suitable for use as light-weight EMI shielding materials.

Acknowledgements

WMZ acknowledges the support from Overseas Research Scholarship Award Scheme and the University of Bristol Postgraduate Scholarship. Mr Jones of School of Chemistry, University of Bristol, helped with the TEM imaging.

References

[1] H. Xu, S. Zhang, S.M. Anlage, L. Hu and G. Gruner, *Frequency- and electric-field-dependent conductivity of single-walled carbon nanotube networks of varying density*, Phys. Rev. B 77, 075418 (2008), pp. 1–6.
[2] Z. Wu, Z. Chen, X. Du, J.M. Logan, J. Sippel, M. Nikolou, K. Kamaras, J.R. Reynolds, D.B. Tanner, A.F. Hebard, and A.G. Rinzler, *Transparent, conductive carbon nanotube films*, Science 305 (2004), pp. 1273–1276.
[3] H. Dai, *Carbon nanotubes: Opportunities and challenges*, Surf. Sci. 500 (2002), pp. 218–241.
[4] H.C. Lee, J. Kim, C.-H. Noh, K.Y. Song and S.-H. Cho, *Selective metal pattern formation and its EMI shielding efficiency*, Appl. Surf. Sci. 252 (2006), pp. 2665–2672.

[5] Q.W. Li, Y. Li, X. Zhang, S.B. Chikkannanavar, Y. Zhao, A.M. Dangelewicz, L. Zheng, S.K. Doorn, Q. Jia, D.E. Peterson, P.N. Arendt and Y.T. Zhu, *Structure-dependent electrical properties of carbon nanotube fibers*, Adv. Mater. 19 (2007), pp. 3358–3363.
[6] J.M. Planeix, N. Coustel, B. Coq, V. Brotons, P. S. Kumbhar, R. Dutartre, P. Geneste, P. Bernier, and P.M. Ajayan, *Application of carbon nanotubes as supports in heterogeneous catalysis*, J. Am. Chem. Soc. 116 (1994), pp. 7935–7936.
[7] F. Wang, S. Arai, and M. Endo, *Metallization of multi-walled carbon nanotubes with copper by an electroless deposition process*. Electrochem. Comm. 6 (2004), pp. 1042–1044.
[8] A.V. Ellis, K. Vijayamohanan, R. Goswami, N. Chakrapani, L.S. Ramanathan, P.M. Ajayan and G. Ramanath, *Hydrophobic anchoring of monolayer-protected gold nanoclusters to carbon nanotubes*, Nano Lett. 3 (2003), pp. 279–282.
[9] B.M. Quinn, C. Dekker, and S.G. Lemay, *Electrodeposition of noble metal nanoparticles on carbon nanotubes*, J. Am. Chem. Soc. 127 (2005), pp. 6146–6147.
[10] Y. Zhang, N.W. Franklin, R.J. Chen and H. Dai, *Metal coating on suspended carbon nanotubes and its implication to metal–tube interaction*, Chem. Phys. Lett. 331 (2000), pp. 35–41.
[11] K. Kendall, *Shrinkage and peel strength of adhesive joints*, J. Phys. D Appl. Phys. 6 (1973), pp. 1782–1787.
[12] A. Kis, G. Csányi, J.-P. Salvetat, Thien-Nga Lee, E. Couteau, A.J. Kulik, W. Benoit, J. Brugger and L. Forró, *Reinforcement of single-walled carbon nanotube bundles by intertube bridging*, Nat. Mater. 3 (2004), pp. 153–157.
[13] P.C. Hiemenz and R. Rajagopalan, *Principles of Colloid and Surface Chemistry*, CRC Press, 1997.
[14] M.J. Rosen, *Surfactants and Interfacial Phenomena*, John Wiley and Sons, 2004.
[15] M.J. O'Connell, S.M. Bachilo, C.B. Huffman, V.C. Moore, M.S. Strano, E.H. Haroz, K.L. Rialon, P.J. Boul, W.H. Noon, C. Kittrell, J. Ma, R.H. Hauge, R.B. Weisman, R.E. Smalley, *Band gap fluorescence from individual single-walled carbon nanotubes*, Science 297 (2002), pp. 593–596.
[16] H. Jiang, L. Zhu, K. Moon and C.P. Wong, *The preparation of stable metal nanoparticles on carbon nanotubes whose surfaces were modified during production*, Carbon 45 (2007), pp. 655–661.
[17] D. Kuang, A. Xu, Y. Fang, H. Ou and H. Liu, *Preparation of inorganic salts ($CaCO_3$, $BaCO_3$, $CaSO_4$) nanowires in the Triton X-100/cyclohexane/water reverse micelles*, J. Cryst. Growth 244 (2002), pp. 379–383.
[18] M.T. Byrne, Y.R. Hernandez, T. Conaty, F.M. Blighe, J.N. Coleman and Y.K. Gun'ko, *Preparation of buckypaper–copper composites and investigation of their conductivity and mechanical properties*, ChemPhysChem 10 (2009), pp. 774–777.
[19] N.F. Colaneri, and L.W. Shacklette, *EMI shielding measurements of conductive polymer blends*, IEEE Trans. Instrum. Meas. 41 (1992), pp. 291–297.
[20] J. Joo and C.Y. Lee, *High frequency electromagnetic interference shielding response of mixtures and multilayer films based on conducting polymers*, J. Appl. Phys. 88 (2000), pp. 513–518.
[21] Y. Yang, M.C. Gupta, and K.L. Dudley, *Towards cost-efficient EMI shielding materials using carbon nanostructure-based nanocomposites*, Nanotechnology 18 (2007), 345701.
[22] X. Shui and D.D.L. Chung, *Nickel filament polymer-matrix composites with low surface impedance and high electromagnetic interference shielding effectiveness*, J. Electron. Mater. 26 (1997), pp. 928–934.
[23] W.A. deHeer, W.S. Bacsa, A. Châtelain, T. Gerfin, R. Humphrey-Baker, L. Forro and D. Ugarte, *Aligned carbon nanotube films: Production and optical and electronic properties*, Science 268 (1995), pp. 845–847.